journal

J. Am. Ceram. Soc., **84** [1] 193–99 (2001)

Crystallization Behavior of Sol–Gel-Derived Strontium Barium Niobate Thin Films

Junmo Koo, Jae Hyeok Jang, and Byeong-Soo Bae

Laboratory of Optical Materials and Coating (LOMC), Department of Materials Science and Engineering, Korea Advanced Institute of Science and Technology (KAIST), Taejon 305-701, Korea

The crystallization of sol–gel-derived strontium barium niobate (SBN) thin films on various substrates is enhanced by a two-step heating process. Also, SBN films with *c*-axis preferred orientation are obtained on MgO (100) substrates. The crystallized phase and the degree of orientation are dependent on crystallization temperature and film composition. The crystallization temperature required to form a single tetragonal tungsten bronze (TTB) SBN phase increases with an increase of Sr content due to the distorted SBN structure. However, in the case of the film on MgO substrate, the oriented crystallization which forms the single tetragonal phase occurs at a lower crystallization temperature than those of polycrystalline films because of lattice matching between the film and the substrate. Its optical and ferroelectric properties were also investigated. They vary depending on film composition, due to the effect of the distorted SBN structure.

I. Introduction

STRONTIUM BARIUM NIOBATE ($Sr_xBa_{1-x}Nb_2O_6$, SBN_{X100}, where $0.25 \leq x \leq 0.75$) is currently being investigated as a potential material for many microdevice applications such as pyroelectric infrared detectors, electrooptic modulators, holographic storage, and beam steering because of its large pyroelectric coefficient, excellent piezoelectric and electrooptic properties, and photorefractive sensitivity.[1–4] Its figure of merit for photorefractive applications is more than 50 times higher than that of $LiNbO_3$, offering the possibility of much smaller devices.[2,4] SBN is a ferroelectric solid solution between $BaNb_2O_6$ and $SrNb_2O_6$ phases with a tetragonal tungsten bronze (TTB) structure, and its physical properties vary with its composition.[5,6]

Although SBN single crystals have been grown mainly by the Czochralski method, it is usually difficult except for the congruent melt composition at $x = 0.6$. Another difficulty is attributed to the high calcination temperature (>1150°C).[6] Recently, the demand for thin film processing has increased because of the development of integrated devices and low processing temperature. SBN thin films, especially highly *c*-axis-oriented SBN thin films, are desired for optical applications, such as electrooptic properties, photorefractive, and nonlinear optical applications.[3,7,8] Hirano and coworkers synthesized highly *c*-axis-oriented SBN ($x = 0.5$) thin films on an MgO (100) substrate by the sol–gel method.[9,10] However, the other compositions of the SBN film have not been studied.

Sol–gel technique has been developed for ferroelectric thin film processes because of excellent homogeneity, ease of chemical composition control, high purity, low processing temperatures, and film uniformity over a large area. However, sol–gel-derived SBN thin films have rarely been investigated because of difficult preparation of a stable solution and high crystallization temperatures. Preparation of SBN sol with the usual solvents, such as ethanol or 2-propanol, is undesirable because these metal alkoxides are highly susceptible to hydrolysis; therefore, special handling and storage of the SBN sol are required.[9–11] Also, the sol–gel-derived SBN thin film does not crystallize well on a glass substrate.[3,11] Thus, it is difficult to obtain fully densified films, and the quality of the films is not better than the films prepared by pulsed laser deposition or metal organic chemical vapor deposition.

In the present study, for the fabrication of sol–gel-derived SBN thin films with various compositions, we have demonstrated the use of an improved crystallization process which results in easier formation of the ferroelectric tetragonal tungsten bronze (TTB) crystalline phase. The dependence of heating temperature and composition on phase formation and oriented crystallization in the SBN thin films was investigated. The optical and ferroelectric properties of the films were also characterized depending on composition.

II. Experimental Procedure

The three compositions investigated in the present study were $x = 0.25$, 0.60, and 0.75 in the general chemical formula $Sr_xBa_{1-x}Nb_2O_6$. The detailed procedure for preparing the precursor solution is shown in Fig. 1. Strontium metal, barium metal (99%, Aldrich Chemical, USA), and niobium ethoxide (99.95%, Aldrich Chemical) were used as the starting agents. 2-Methoxyethanol (99.9%, Aldrich Chemical) was used as a solvent. 2-Methoxyethanol is a common solvent for many sol–gel-prepared ferroelectric films like the $(Pb,La)(Ti,Zr)O_3$ (PLZT) system, because the oxygen atom in the methoxyethoxy group has more negative partial charge than that in the ethoxy group.[11,12] This property makes 2-methoxyethanol a better nucleophilic solvent than ethanol. Thus, 2-methoxyethanol stabilizes the SBN solution. Strontium metal and barium metal, corresponding to the desired stoichiometric ratio of the SBN, were dissolved in 2-methoxyethanol and refluxed at 120°C for 6 h. This solution was then heated at 80°C for 6 h to distill undesired organic compounds. A niobium solution was made by a similar process. The final solution, which had a concentration of 0.1*M*, was clear brown without any suspended particles. This solution could be stored for several months because of the effects of the solvent and the low concentration. However, this procedure should be done in a dry nitrogen gas atmosphere because the starting materials are extremely sensitive to moisture. Each solution was mixed using an ultrasonic machine for 1 min before coating. A thin film is usually made using different substrates, coatings, and heat treatment. Each procedure affects the final quality of the thin films. For the choices of substrates, single-crystal silicon (p-type, (100) oriented wafer), fused silica, and single-crystal magnesium oxide were used. Fused silica was chosen because of the absence of ionic impurities and its transparency in the UV spectrum region. Transparent MgO (100)

S.-I. Hirano—contributing editor

Manuscript No. 189008. Received October 18, 1999; approved July 27, 2000.
Supported by the Korea Science and Engineering Foundation, Korea, under Grant No. 981-0803-019-2, and by the Brain Korea 21 project.
*Member, American Ceramic Society.

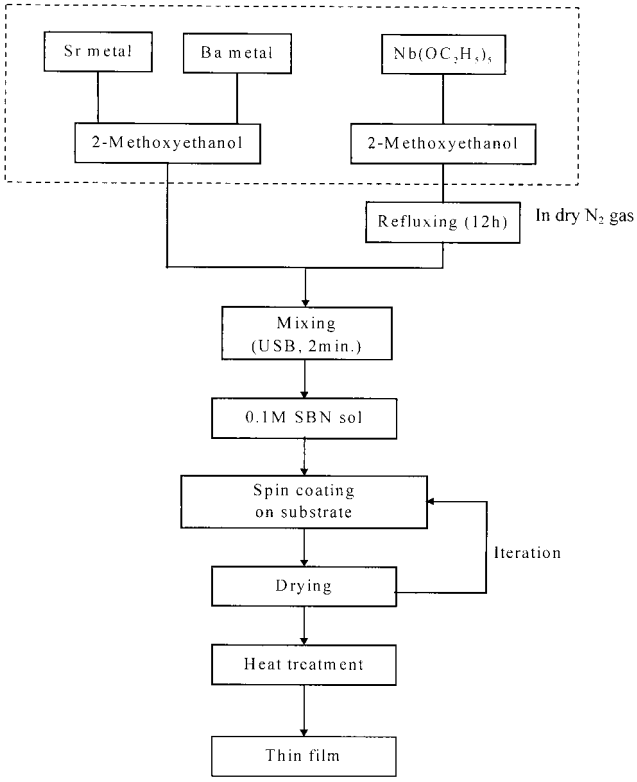

Fig. 1. Flow chart for fabrication of SBN thin films.

single crystal shows good lattice matching with SBN crystal, which can grow an epitaxial SBN layer.[7–11] Also, because the refractive index of MgO is lower than that of SBN, the SBN films on MgO substrates can be fabricated as planar optical waveguides. A silicon wafer, which is a general substrate for the electrical characterization of thin films, was used to compare crystallization behaviors with other studies. However, the surface morphologies of the SBN thin films on silicon substrates heat-treated at 1000°C seem not to be good because of the out-diffusion of elemental Si and then the formation of hillock from the high heating temperature. Thus, these films were used only for the analysis of crystalline phases. It was confirmed by Auger electron spectroscopy (AES) that the undesired reaction between a film and a substrate did not occur in the films on the other substrates heat-treated at 1000°C. Pt (100)/MgO (100) substrate where the platinum was sputtered as an electrode was used for the ferroelectric characterization of the oriented thin films.

The mixed solution was spin-coated on these substrates using a spin coater at 2000 rpm for 30 s. After air drying for 5 min, the green film was dried at 180° and 360°C for 10 min on a hot plate, respectively. A coating yielded a film thickness of about 500 Å. This procedure was repeated until the desired thickness was obtained. The films were crystallized at temperatures between 700° and 1000°C for 1 h. The heating rate was 2°C/min to prevent microcracks from thermal shock and rapid shrinking. These films were heat-treated using a new heating schedule, a two-step heating process. The two-step heating process applies the additive heat treatment at 550°C for 5 h before crystallization to enhance the crystallization as well as densification of the films. The effect of the two-step heating process will be described later.

The crystalline phase and microstructure of the films were characterized by X-ray diffraction (Rigaku, D/MAX-RC) and scanning electron microscopy (Phillips 535M). The crystalline phase of the films was also analyzed using transmission electron microscopy (Carl Zeiss, EM912Ω). Optical transmission of the films was measured using a UV/vis spectrophotometer (HP 8452P). Measurements of refractive index and thickness of the films were performed with a prism coupler at a wavelength of 632.8 nm. Polarization–electric field (*P–E*) hysteresis of films was obtained using the charge mode in the standard ferroelectric test system (Radiant Technologies, RT66A).

III. Results and Discussion

(1) Preparation of SBN Thin Films

According to previous reports, the crystallization of sol–gel-derived SBN thin films is dependent on the substrate.[3,11] The SBN film on a fused silica substrate has rarely been crystallized at 700°C although the film on a silicon substrate can be crystallized at the same temperature.[11] Compared with a crystalline substrate, an amorphous substrate lacks the nucleation sites for the crystallization of the SBN phase. Thus, for the crystallization of the SBN thin films on an amorphous substrate such as a fused silica substrate, a higher temperature is required along with a special heating process, i.e., a two-step heating process. In the two-step heating process, the films are heated from room temperature to 550°C with a slow heating rate (=2°C/min) and maintained at 550°C for 5 h to enhance the densification and the nucleation of the films. Then, the temperature is raised to the crystallization temperature using the same heating rate. Figure 2 shows XRD patterns of SBN60 films on fused silica and silicon substrates that were crystallized at 1000°C with the conventional, single-step heating process and the two-step heating process, respectively. As shown in Fig. 2(a), the film on a fused silica substrate processed using the single-step heating process is not crystallized even at 1000°C, while the film made using the two-step heating process represents crystalline peaks. The film made using the two-step heating process contained the tetragonal phase with a small amount of undesired orthorhombic phase. This behavior is caused by lower thermal conduction of a fused silica glass than that of a silicon substrate. However, in the case of films on silicon substrates as shown in Fig. 2(b), the films were crystallized with only

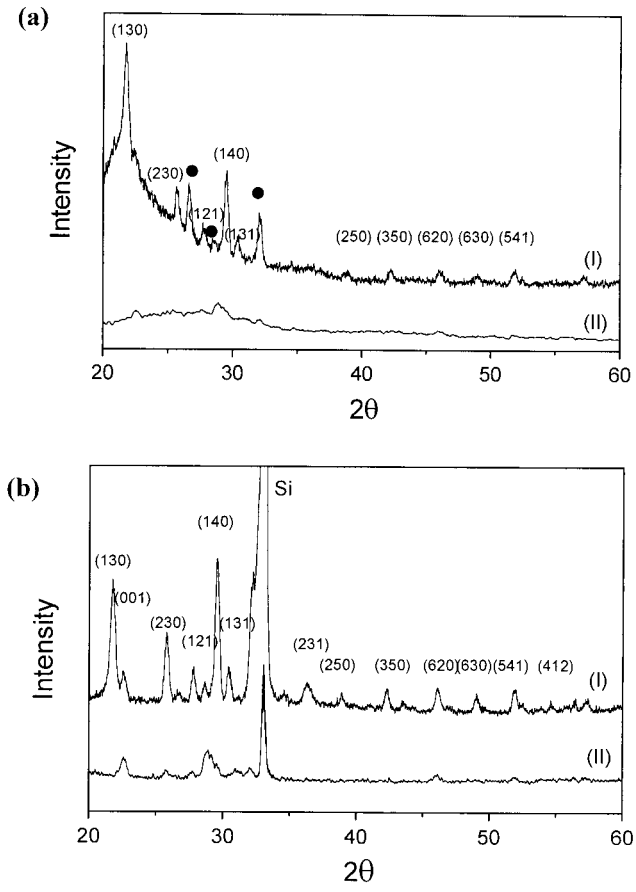

Fig. 2. XRD patterns of SBN60 thin films on (a) fused silica substrates and (b) silicon substrates crystallized at 1000°C by different heating processes.

tetragonal phase regardless of the heating processes. Also, it is shown that the film made using the two-step heating is more crystallized. Thus, it is found that the crystallization of the SBN film, especially on an amorphous substrate, is affected by the degree of crystallization of the substrate. In addition, the crystallization of the film is promoted when more nucleation sites in the films are created by preheating in the two-step heating process.

Figure 3 shows SEM micrographs of SBN60 thin films on fused silica substrates crystallized at 1000°C with single- and two-step heating processes, respectively. The surface morphology and the cross section of the film using a single-step heating process are relatively rough and loose. On the other hand, the surface morphology of the film prepared by the two-step heating process is crack-free and uniform, and has a small grain size (0.3–0.5 μm), as shown in Fig. 3(a). In Fig. 3(b), the film prepared by the two-step heating process not only has many spherical grains but also has a dense and clean cross section, while the film using the single-step heating process exhibits pores in the whole cross section of the film. This is because the preheating (heating at 550°C for 5 h) creates more nucleation sites leading to full densification and crystallization. Thus, the two-step heating process is more effective in obtaining good crystalline sol–gel films for practical applications. All of the SBN thin films studied in this study were prepared by applying the two-step heating process.

(2) Formation of Tetragonal Tungsten Bronze (TTB) Phase

Studies have been made of the phase formation during the crystallization of sintered SBN crystal.[6,13,14] Intermediate phases such as $Ba_5Nb_4O_{15}$ and $Sr_5Nb_4O_{15}$ start to develop at about 600°C and are fully formed below 900°C. Between 800° and 1000°C, metastable phases such as $BaNb_2O_6$ and $SrNb_2O_6$ are well developed as $Ba_5Nb_4O_{15}$ and $Sr_5Nb_4O_{15}$ disappear. Then, the former two phases, $BaNb_2O_6$ and $SrNb_2O_6$, react to form a TTB SBN phase. The low-temperature binary phases, i.e., $Ba_5Nb_4O_{15}$, $Sr_5Nb_4O_{15}$, $BaNb_2O_6$, and $SrNb_2O_6$, are known as paraelectric phases. Only the TTB SBN phase is ferroelectric. However, in the case of the thin films, the exact formation temperature of the TTB SBN phase has not been reported.

Figure 4 illustrates XRD patterns of the SBN films on silicon substrates as a function of crystallization temperature and film composition. All of the films heat-treated at 700°C crystallize as an orthorhombic phase, which is similar to the $SrNb_2O_6$ (SN) or $BaNb_2O_6$ (BN), but the TTB SBN phase begins to form at 800°C. As mentioned above, in the crystallization of bulk SBN crystal, the intermediate phases such as $Ba_5Nb_4O_{15}$ and $Sr_5Nb_4O_{15}$, and the metastable phases such as $BaNb_2O_6$ and $SrNb_2O_6$, are developed at lower temperature. The latter two phases react to form TTB SBN phase. However, the intermediate phases are not observed in the XRD patterns of the sol–gel-derived SBN films. Thus, the TTB SBN phase is formed by the reaction of only the orthorhombic strontium niobate (SN) and barium niobate (BN) phases without developing the intermediate phases. It is also found that the behavior depends on the film composition. The SBN films on silicon substrates with higher Sr content start to transform from the mixed orthorhombic phases to the single TTB phase at a higher crystallization temperature as shown in Fig. 4. In the case of the SBN25 and SBN60 compositions, the films transform perfectly to single TTB SBN phase over 900°C. However, the SBN75 film crystallizes at 1000°C to form single TTB phase. Based on the structure of the SBN unit cell, the following explanation of this behavior is proposed. The compositional dependence on the single TTB phase formation temperature might be correlated with higher lattice distortion in the tungsten bronze structure for greater Sr content in the SBN composition. In the unit cell of the TTB SBN structure, A_1 sites are occupied only by Sr^{2+} ions whereas A_2 sites are occupied by both Ba^{2+} and Sr^{2+} ions, as shown in Fig. 5.[5] As the fraction of Sr^{2+} ion content increases, more Sr^{2+} ions occupy the A_2 sites and the A_1 sites become empty.[15] Thus, the lattice will be more distorted.[13–15] The more distorted lattice makes it difficult to transform from the orthorhombic phase to the tetragonal phase because energies such as thermal energy for diffusion of ions in the layers of SBN structure are more needed. Therefore, the SBN film having higher Sr content needs higher thermal energy for the transformation from orthorhombic SN and BN phases to TTB SBN phase.

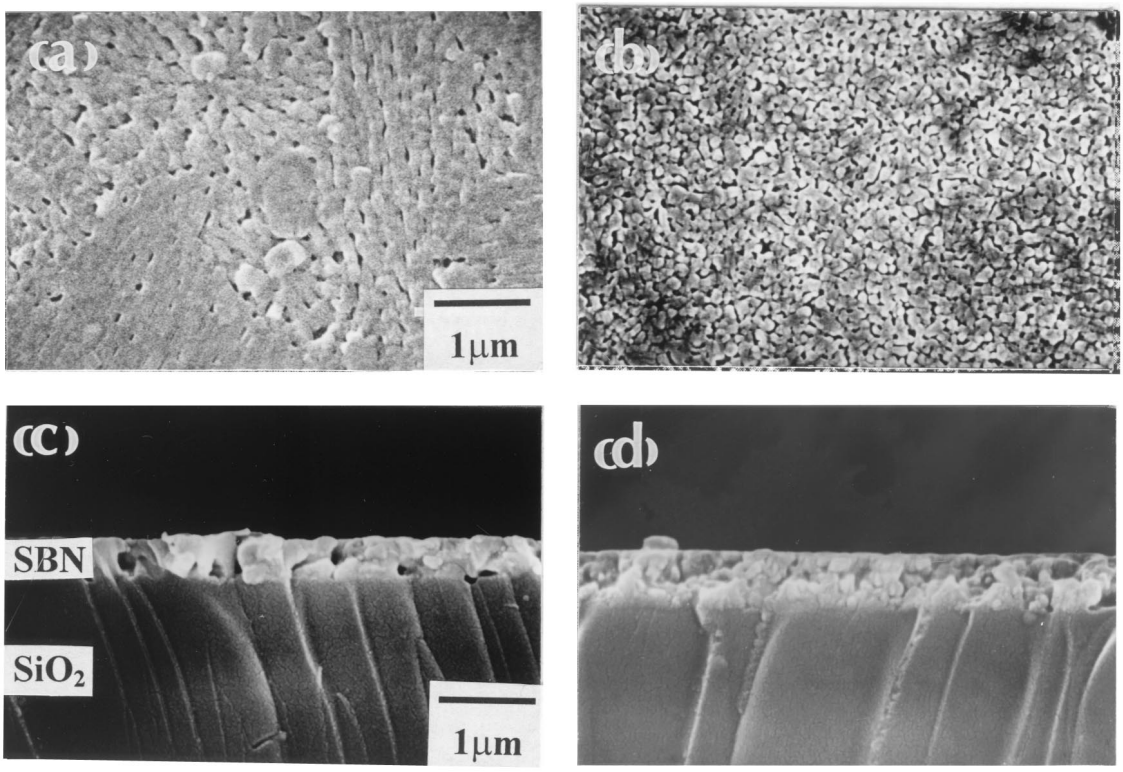

Fig. 3. Plane-view and cross-sectional SEM micrographs of SBN60 thin films on fused silica substrates prepared by (a,c) a single heating process, and (b,d) a two-step heating process.

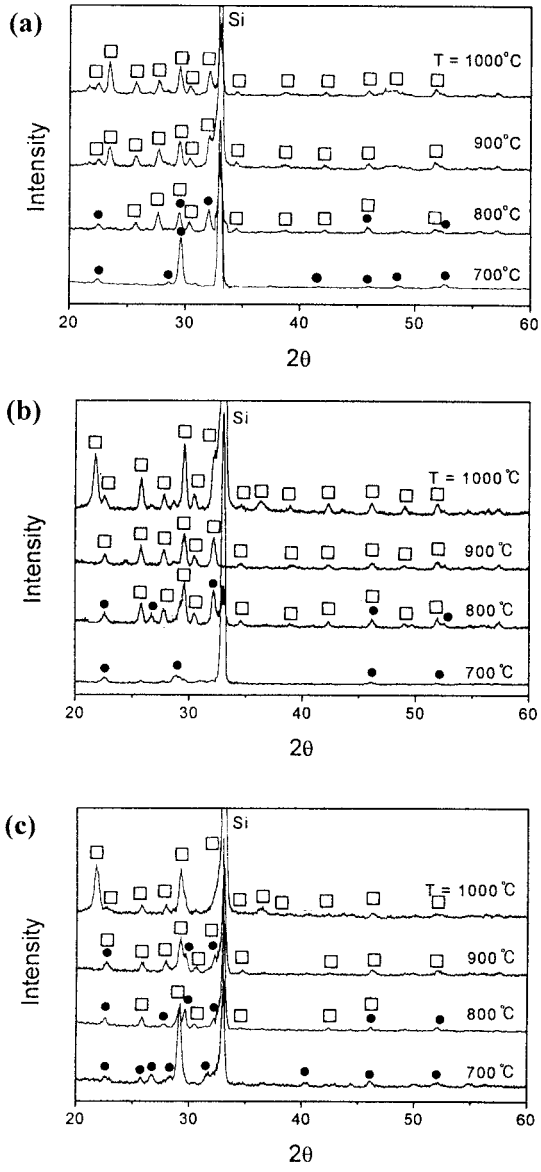

Fig. 4. XRD patterns of SBN thin films on silicon substrates with different compositions prepared as a function of crystallization temperature: (a) SBN25, (b) SBN60, and (c) SBN75.

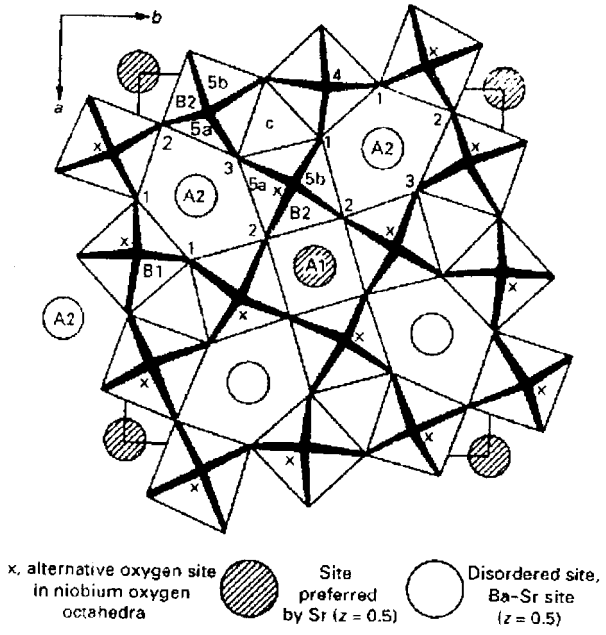

Fig. 5. Atomic arrangement in unit cell of tungsten bronze type of SBN structure projected along the polar *c*-axis.

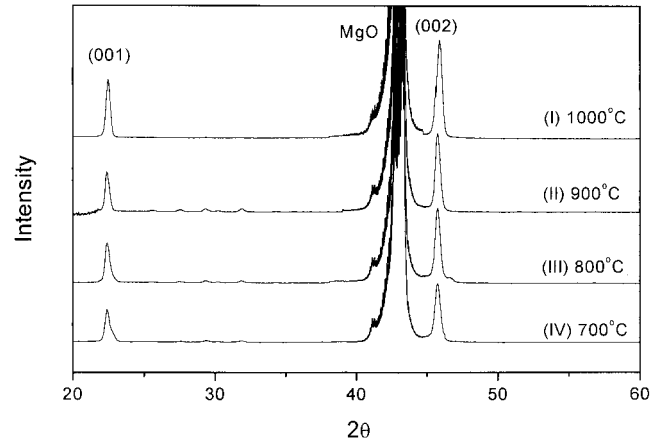

Fig. 6. XRD patterns of SBN60 thin films on MgO (100) substrates as a function of crystallization temperature.

(3) Oriented Crystallization of SBN Films

Figure 6 shows XRD patterns of the SBN60 thin films on MgO (100) substrates crystallized at various temperatures between 700° and 1000°C. All of the films are crystallized with preferred *c*-axis orientation, but the intensity of the XRD peaks is enhanced with increasing crystallization temperature. However, for the phase of the films crystallized below 900°C it cannot be determined whether a mixed phase or only the tetragonal phase is present, according to the result of polycrystalline SBN thin films on silicon substrates, since the position of the (001) XRD peak in Fig. 6 is seldom identical for the tetragonal and orthorhombic phases.[9] For the *c*-axis-oriented SBN films on MgO substrates, TEM diffraction of the films crystallized at 700° and 1000°C was examined to understand the dependence of the phase transition on crystallization temperature. A TEM diffraction image is widely used to analyze the structure of a crystalline phase. TEM diffraction patterns of the (001) plane of SBN films on MgO substrates are presented in Fig. 7. A faint dispersed ring pattern is shown for the film crystallized at 700°C (Fig. 7(a)) but not for the film crystallized at 1000°C (Fig. 7(b)) because of its having a larger grain size and uniform grain arrangement by high crystallization temperature. However, no distinct difference can be found in the spot position as well as the distance between the spots, comparing Figs. 7(a) and (b). According to calculations, the axes *a* and *b* of the SBN unit cell in Fig. 7 have equal lengths. This result suggests that the phases of the SBN films crystallized at both 700° and 1000°C are the same as the single tetragonal SBN phase, not the orthorhombic phase. Thus, the lattice matching of the SBN and MgO structures enhances the crystallization of the SBN film enough to form the single TTB SBN phase even at low crystallization temperatures as low as 700°C. However, the preferred oriented crystallization is enhanced by increasing the crystallization temperature. This could be confirmed in the rocking curves of the (001) XRD peak depending on the crystallization temperature as shown in Fig. 8. The full width at half-maximum (FWHM) values of the rocking curves as presented in the inset of Fig. 8 decreases as the crystallization temperature increases. Also, the maximum peak of the rocking curves shifts to low angle with increasing crystallization temperature due to the grain growth of SBN films from 0.1 μm to 0.5 μm, which was observed in plain-view TEM micrographs. For the oriented crystallized film, the nucleation which occurs at the interface between a film and a lattice-matching substrate would lead to the formation of a highly preferred oriented film.[7,8,18] Thus, raising the crystallization temperature maximizes

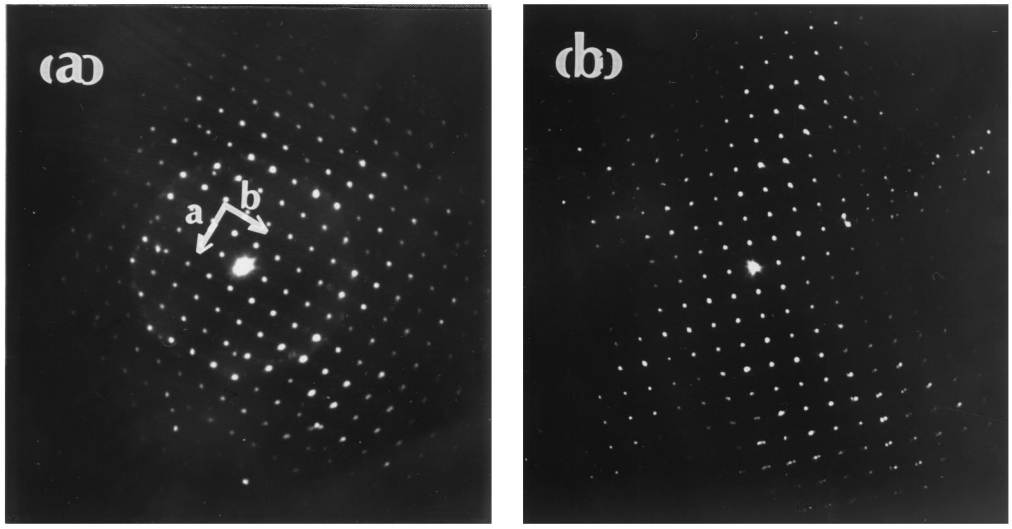

Fig. 7. Selected area diffraction patterns of (001) plane in SBN thin films on MgO (100) substrates crystallized at (a) 700° and (b) 1000°C.

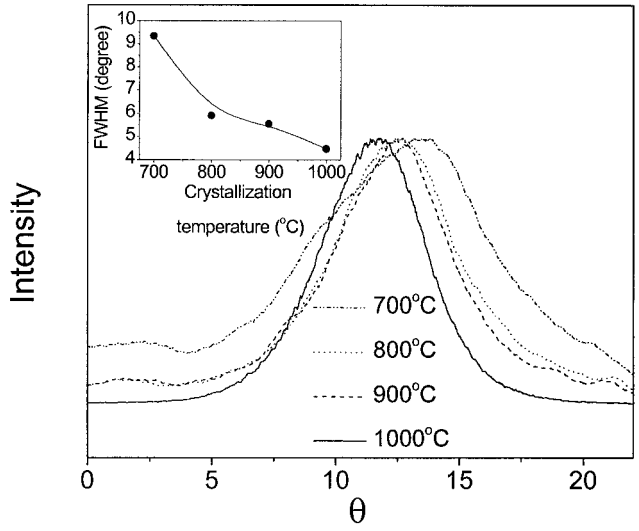

Fig. 8. Rocking curves of SBN60 thin films on MgO (100) substrates as a function of crystallization temperature, where inset is a plot of the full width at half-maximum (FWHM) values.

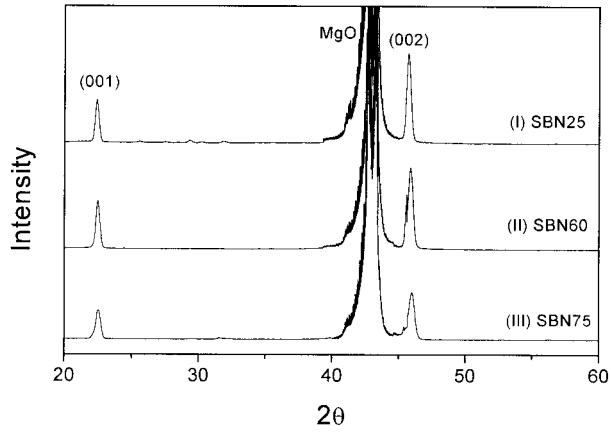

Fig. 9. XRD patterns of SBN thin films on MgO (100) substrates as a function of film composition.

the nucleation between the SBN film and the MgO substrate, and results in better orientation in the film.

Figure 9 shows the XRD patterns of SBN films on MgO (100) substrates with different compositions. All of the films crystallized at 1000°C have the preferred *c*-axis orientation consisting of single TTB SBN phase, regardless of the film composition. From the XRD measurement, the calculated lattice constant along the *c*-axis decreases from 3.941 to 3.832 Å as Sr content increases. The FWHM values in the rocking curves of the (001) XRD peak in these films, as shown in Fig. 10, increase slightly as Sr content in the film composition increases. The variation of the FWHM values depending on the film composition may also be affected by the more distorted lattice with an increase of Sr content, which is similar to previous results. Thus, it is found that the SBN film with higher Sr content has more distorted structure presenting lower quality orientation of the films on the MgO substrate.

(4) Optical Properties of SBN Films

The optical transmission spectra of the SBN films on fused silica substrates are shown in Fig. 11. Fused silica substrate is proper to measure the absorption edge of the film, because it has the transparency in the UV spectrum region. All the films are highly transparent in the wavelength range from 0.2 to over 1.4 μm, but the absorption edges of the films are dependent on the film composition. The absorption edge of the SBN film on a fused silica substrate decreases slightly with an increase of Sr content, as shown in the inset of Fig. 11. The dependency of the absorption edge on the composition is similar to that of single crystals. It has been reported that the absorption edges of single crystals SBN50 and SBN60 are 350 and 250 nm, respectively.[17] These values are greater than those observed in this study since the absorption edge is sensitive to the thickness of sample as well as processing.

Figure 12 shows the refractive indexes of *c*-axis-oriented SBN films on MgO (100) substrates as a function of film composition. This figure shows that SBN is an optically uniaxial negative material ($n_0 > n_e$). The ordinary refractive index, n_0, increases as the Sr content in the film composition decreases due to an increase of BaO, which has a higher refractive index. However, the extraordinary index, n_e, is more sensitive than the ordinary index to changes in the film composition, because n_e is affected by electronic and ionic polarization, changes in the lattice parameter, and structure, whereas n_0 is affected only by electronic polarization.[18] Thus, the cause of the decrease of n_e with increasing Sr content in the film is more complicated. The refractive indexes of the films approach that of single-crystal SBN, which reflects that the films are fully densified.[2,3,18] In addition, birefringence, Δn ($=n_0 - n_e$), decreases as Sr content in the film composition decreases.

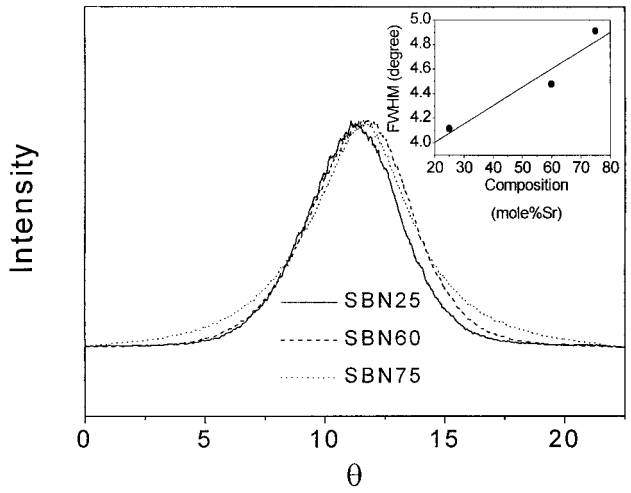

Fig. 10. Rocking curves of SBN thin films on MgO (100) substrates as a function of film composition, where inset is a plot of the full width at half-maximum (FWHM) values.

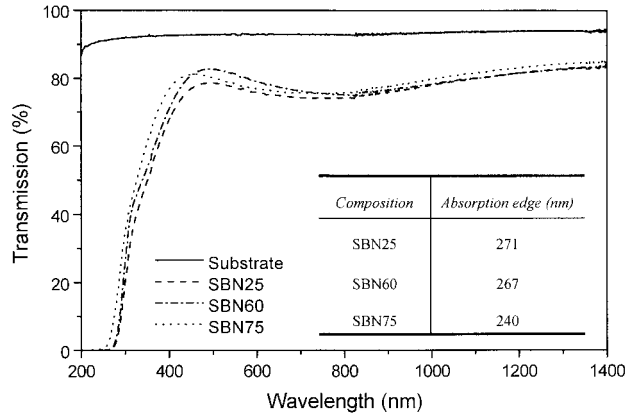

Fig. 11. Optical transmission spectra of SBN thin films (3000 Å) on fused silica substrates as a function of film composition. Inset is a table of the absorption edges of SBN films.

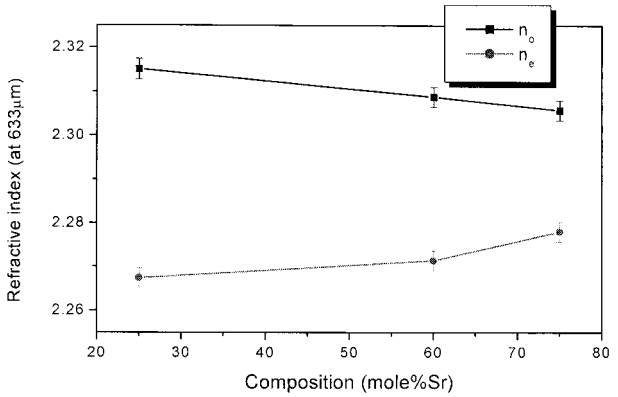

Fig. 12. Refractive index of SBN thin films on MgO (100) substrates as a function of film composition.

(5) P–E Hysteresis of SBN Thin Film

Polarization–electric field (*P–E*) hyteresis loops were obtained for the SBN thin films with different compositions on a Pt (100)/MgO (100) substrate with metal–insulator–metal (MIM) structure. SBN thin films on Pt (100)/MgO (100) substrates exhibit *c*-axis orientations, as reported in a previous report.[10] Figure 13 shows the *P–E* hysteresis loops of the oriented SBN thin films.

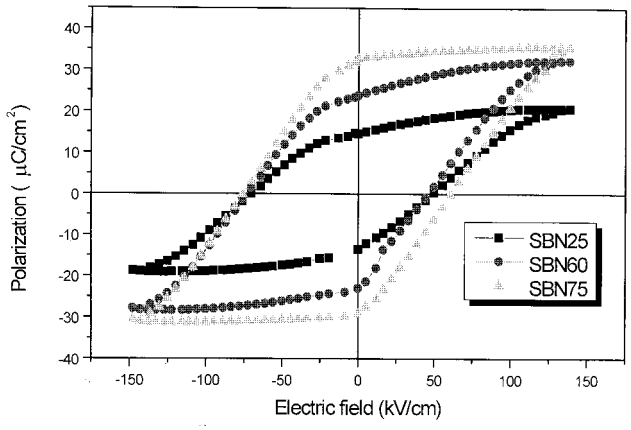

Fig. 13. *P–E* hysteresis loops of SBN thin films (5000 Å) on Pt/MgO substrates as a function of film composition.

Both remanent polarization (P_r) and coercive field (E_c) values of the SBN films increase as Sr content in the film composition increases. The variation of P_r depending on the composition can be illustrated by the ferroelectric mechanism of SBN material. In the unit cell of the SBN lattice, the displacement of the Nb^{5+} ion is the dominant mechanism for producing polarization, and the displacement of Sr^{2+} ion in the A_2 site is more important than that in the A_1 site.[5] Because the area of the A_2 site is larger than that of the A_1 site and the radius of the Ba^{2+} ion is larger than that of the Sr^{2+} ion, Sr^{2+} ions rather than Ba^{2+} ions in A_2 sites are free to move along the direction of the applied external electric field. Since the number of Sr^{2+} ions in the A_2 sites increases when the Sr/Ba ratio in the film increases, the polarization ($\sim P_r$) can increase relatively as Sr content increases. The increase of E_c values with an increase of Sr content might be correlated with the increase of lattice distortion in the tungsten bronze structure as Sr content is raised in the SBN composition. Since Nb octahedra in the distorted lattice are more dislocated from the *c*-axis of the tetragonal structure as Sr content increases, the distorted lattice makes it difficult for permanent dipoles to change the direction of polarization along the applied electric field. Thus, energy from the electric field is more necessary as Sr content increases.

IV. Conclusions

Dense, crack-free, and transparent SBN films on fused silica, silicon wafer, and MgO(100) substrates were prepared by the sol–gel method using a two-step heating process. The preferred *c*-axis orientation was observed for SBN films on MgO (100) substrates. The two-step heating process, including preheating, enhanced the crystallization and the densification of SBN films. The binary orthorhombic phases crystallized at low temperature were transformed to single-phase TTB SBN with increasing temperature. The transition temperature needed to form a single phase in the SBN film increased with increasing Sr content. This occurs because the higher Sr content causes more distortion, requiring higher thermal energy for transformation to the tetragonal structure. The more distorted structure of SBN film with increasing Sr content was confirmed by the change of the rocking curve for the *c*-axis-oriented SBN films on MgO (100) substrates. However, the SBN films on MgO substrates produced a single TTB SBN phase regardless of the crystallization temperature, because lattice-matching between the film and the substrate enhances crystallization in the SBN film. The absorption edge of the films shifted to shorter wavelength and the refractive index decreased as Sr content grew. Also, the ordinary and extraordinary indexes of *c*-axis-oriented SBN films on MgO substrates show the opposite behavior as Sr content increases. Both the remanent polarization (P_r) and the coercive field (E_c) of the *c*-axis-oriented SBN thin films increased as Sr content increased because of the greater displacement of Sr ions and the distorted structure, respectively.

References

[1]A. M. Glass, "Investigation of the Electrical Properties of $Sr_{1-x}Ba_xNb_2O_6$ with Special Reference to Pyroelectric Detection," *J. Appl. Phys.*, **40** [12] 4699–713 (1969).

[2]R. R. Neurgaonkar, W. F. Hall, J. R. Oliver, W. W. Ho, and W. K. Cory, "Tungsten Bronze $Sr_{1-x}Ba_xNb_2O_6$: A Case History of Versatility," *Ferroelectrics*, **87**, 167 (1988).

[3]Y. Xu, C. J. Chen, R. Xu, and J. D. Mackenzie, "Ferroelectric $Sr_{0.60}Ba_{0.40}Nb_2O_6$ Thin Films by the Sol–Gel Process: Electrical and Optical Properties," *Phys. Rev. B*, **44** [1] 35–41 (1991).

[4]P. V. Lenzo, E. G. Spencer, and A. A. Ballman, "Electro-optic Coefficients of Ferroelectric Strontium Barium Niobate," *Appl. Phys. Lett.*, **11** [1] 23–24 (1967).

[5]P. B. Jamieson, S. C. Abrahams, and J. L. Bernstein, "Ferroelectric Tungsten Bronze-Type Crystal Structures. I. Barium Strontium Niobate $Ba_{0.27}Sr_{0.75}Nb_2O_{5.78}$," *J. Chem. Phys.*, **48** [11] 5048–57 (1968).

[6]N. S. VanDamme, A. E. Sutherland, L. Jones, K. Bridger, and S. R. Winzer, "Fabrication of Optically Transparent and Electrooptic Strontium Barium Niobate Ceramics," *J. Am. Ceram. Soc.*, **74** [8] 1785–92 (1991).

[7]S. S. Thöny, K. E. Youden, J. S. Harris Jr., and L. Hesselink, "Growth of Epitaxial Strontium Barium Niobate thin Films by Pulsed Laser Deposition," *Appl. Phys. Lett.*, **65** [16] 2018–20 (1994).

[8]M. Lee and R. S. Feigelson, "Growth of Epitaxial Strontium Barium Niobate Thin Films by Soild Source Metal-organic Chemical Vapor Deposition," *J. Cryst. Growth*, **180**, 220–28 (1997).

[9]S. Hirano, T. Yogo, K. Kikuta, and K. Ogiso, "Preparation of Strontium Barium Niobate by Sol–Gel Method," *J. Am. Ceram. Soc.*, **75** [6] 1697–700 (1992).

[10]W. Sakamoto, T. Yogo, K. Kikuta, K. Ogiso, A. Kawase, and S. Hirano, "Synthesis of Strontium Barium Niobate Thin Films Through Metal Alkoxide," *J. Am. Ceram. Soc.*, **79** [9] 2283–88 (1996).

[11]C. H. Luk, C. L. Mak, and K. H. Wong, "Characterization of Strontium Barium Niobate Films Prepared by Sol–Gel Process Using 2-Methoxyethanol," *Thin Solid Films*, **298**, 57–61 (1997).

[12]J. Koo, S.-U. Kim, D. S. Yoon, K. No, and B.-S. Bae, "Effect of Heat Treatment on Formation of Sol–Gel (Pb,La)TiO_3 Films for Optical Application," *J. Mater. Res.*, **12** [3] 812–18 (1997).

[13]T.-S. Fang, N.-T. Wu, and F.-S. Shiau, "Formation Mechanism of Strontium Barium Niobate Ceramic Powders," *J. Mater. Sci. Lett.*, **13**, 1746–48 (1994).

[14]W.-J. Lee and T.-T. Fang, "Nonisothermal Reaction Kinetics of $SrNb_2O_6$ and $BaNb_2O_6$ for the Formation of $Sr_xBa_{1-x}Nb_2O_6$," *J. Am. Ceram. Soc.*, **81** [1] 193–99 (1998).

[15]M. P. Trubelja, E. Ryba, and D. K. Smith, "A Study of Positional Disorder in Strontium Barium Niobate," *J. Mater. Sci.*, **31**, 1435 (1996).

[16]J. Koo, J. H. Jang, and B. S. Bae, "Highly Oriented (Pb,La)TiO_3 Thin Films Prepared by Sol–Gel Process," *J. Mater. Sci.*, **34** [20] 5075–80 (1999).

[17]R. Xu, Y. Xu, C. J. Chen, and J. D. Mackenzie, "Sol–Gel Processing of Strontium-Barium Niobate Ferroelectric Thin Film," *J. Mater. Res.*, **5** [5] 916 (1990).

[18]L. Venturini, E. G. Spencer, P. V. Lenzo, and A. A. Ballman, "Refractive Indices of Strontium Barium Niobate," *J. Appl. Phys.*, **39**, 343–44 (1968). □